SUPPLEMENTARY DATA

Surface-engineered dual drug-loaded tumor-targeted liposomal nanoparticles to overcome the therapeutic resistance in glioblastoma multiforme.

Ramcharan Singh Angom[1$], Hari Krishnareddy Rachamala[1$], Naga Malleswara Rao Nakka[1], Vijay Sagar Madamsetty[1], Paola Suarez Meade[2], Beatriz I Fernadez Gil[2], Tanmay Kulkarni[1], Raegan Weil[2], Shamit Dutta[1], Enfeng Wang[1], Santanu Bhattacharya[1,3], Krishnendu Pal[1], Alfredo Quinones Hinojosa[2], and Debabrata Mukhopadhyay[1, 3*]

Affiliations:

[1]Department of Biochemistry and Molecular Biology, and [2]Department of Neurosurgery, Mayo Clinic College of Medicine and Sciences, Jacksonville, FL 32224

[3]Department of Bioengineering, Mayo Clinic College of Medicine and Sciences, Jacksonville, FL 32224

[$]Both authors contributed equally.

Containing:

Supplementary Materials and Methods;

Supplementary Figures and Figure legends;

Supplementary Tables.

Formulations	Size (nm)	PDI (%)	Zeta (mV)
Tumor targeting Liposome (TTL)	75.62±1.13	0.158±0.02	20.1±0.16
TTL-E	81.52±.12	0.214±0.003	15.3±0.58
TTL-V	78.91±0.08	0.170±0.004	24.8±0.14
TTL-EV	83.65±.13	0.208±0.011	21.3±0.23

Table S1. Characterization of liposomal drug formulations. A. Hydrodynamic size, polydispersity index (PDI) and zeta potential of empty liposomes (L), or liposomes containing Everolimus (E-L), Vinorelbine (V-L), and combination of Everolimus and Vinorelbine (EV-L).

Formulations	Size (nm)	PDI (%)	Zeta (mV)
Tumor targeting Liposome (TTL)	78±12	0.115±0.002	18.2±0.8
R-L	85±14	0.126±0.003	15.2±0.4
V-L	80±10	0.117±0.004	22.8±0.5
RV-L	88±8	0.128±0.003	22.2±0.7

Table S2. Hydrodynamic size, polydispersity index (PDI) and zeta potential of empty liposomes (L), or liposomes containing Rapamycin (R-L), Vinorelbine (V-L), and combination of Rapamycin and Vinorelbine (RV-L). All the measurements were performed in deionized water at 25 °C.

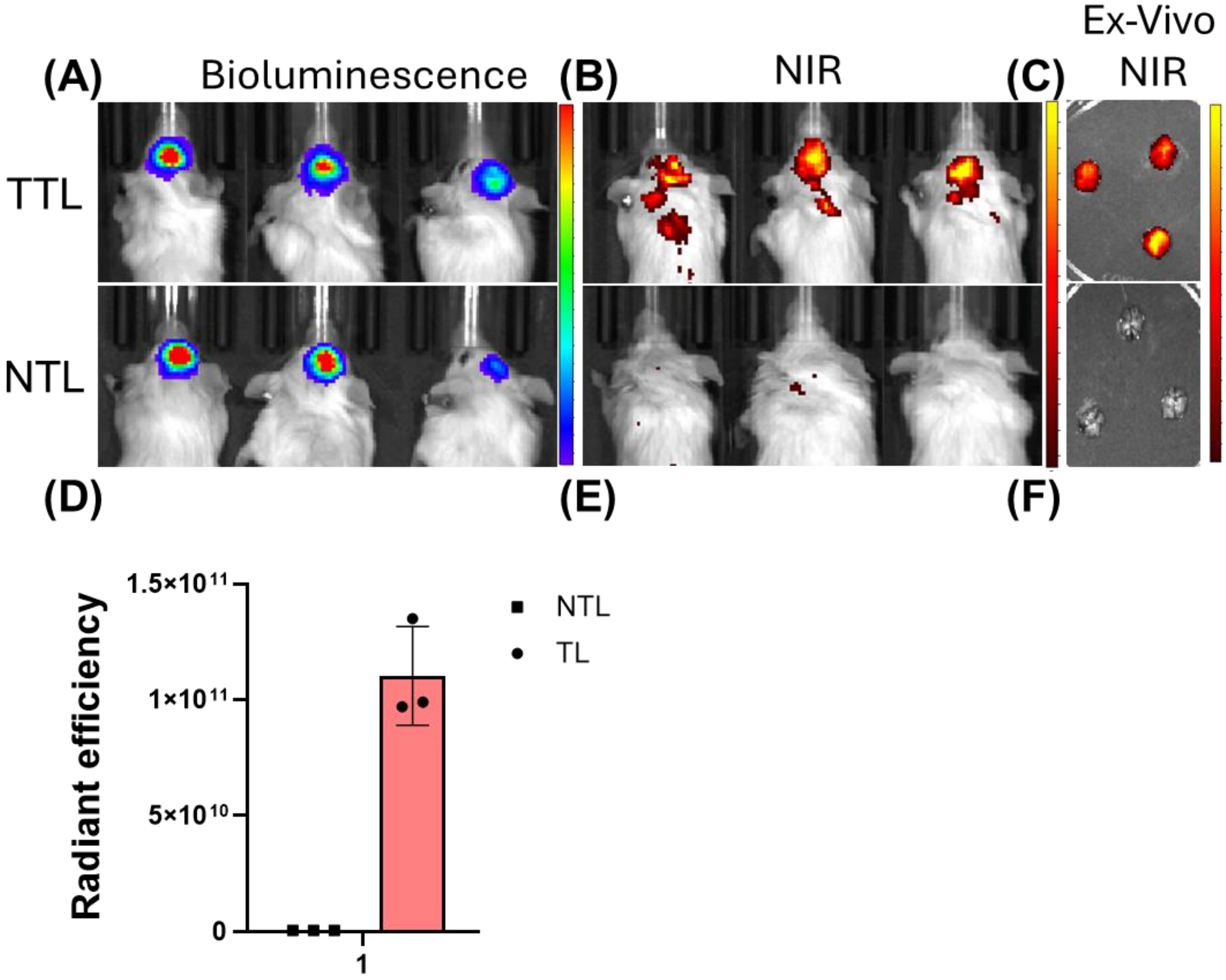

Figure S1. Tumor uptake in GBM Mice: (A) IVIS image of three representative TTL injected mice showing tumor in the brain**. (B)** NIR signals in the brain showing NIR conjugated TTL in the mice brain bearing tumor. **(C)** NIR signal in the dissected brain**. (D)** IVIS image showing tumor in NTL injected mice**. (E-F)** Absence of NIR signal in the NTL injected mice brain in vivo and ex vivo. NTL: Non-Targeted Formulation. And TTL: Tumor Targeted Formulation.

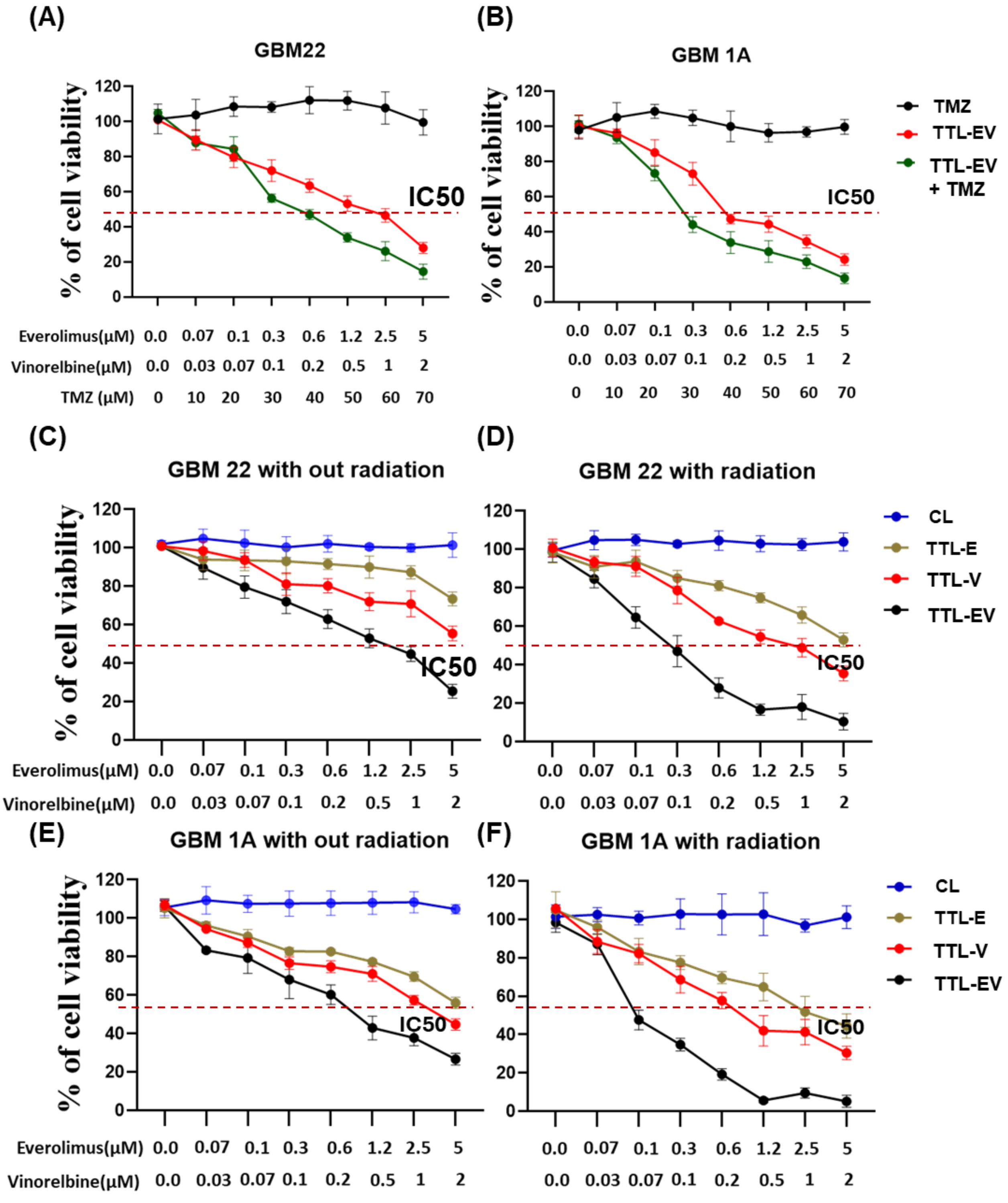
(A)
GBM22
(B)
GBM 1A
% of cell viability
120
100
80
60
40
20
0
IC50
TMZ
TTL-EV
TTL-EV + TMZ
Everolimus(μM) 0.0 0.07 0.1 0.3 0.6 1.2 2.5 5
Vinorelbine(μM) 0.0 0.03 0.07 0.1 0.2 0.5 1 2
TMZ (μM) 0 10 20 30 40 50 60 70
(C)
GBM 22 with out radiation
(D)
GBM 22 with radiation
CL
TTL-E
TTL-V
TTL-EV
(E)
GBM 1A with out radiation
(F)
GBM 1A with radiation

Figure S2. In vitro cellular cytotoxicity of the dual drug-loaded liposomal nanoparticles (TTL-E, TTL-V, TTL-EV) in combination with (A-B) Standard chemotherapeutic drugs (temozolomide (TMZ) in **(A)** GBM22 and **(B)** GBM 1A cell lines. **(C)** without Radiation in GBM 22 cell lines. **(D)** with Radiation in GBM 22 cell lines. **(E)** without Radiation in GBM1A and **(F)** with Radiation in GBM 1A.. Each data point represents the quadruplet results obtained from a single experiment. The dashed line represents the IC50 values.

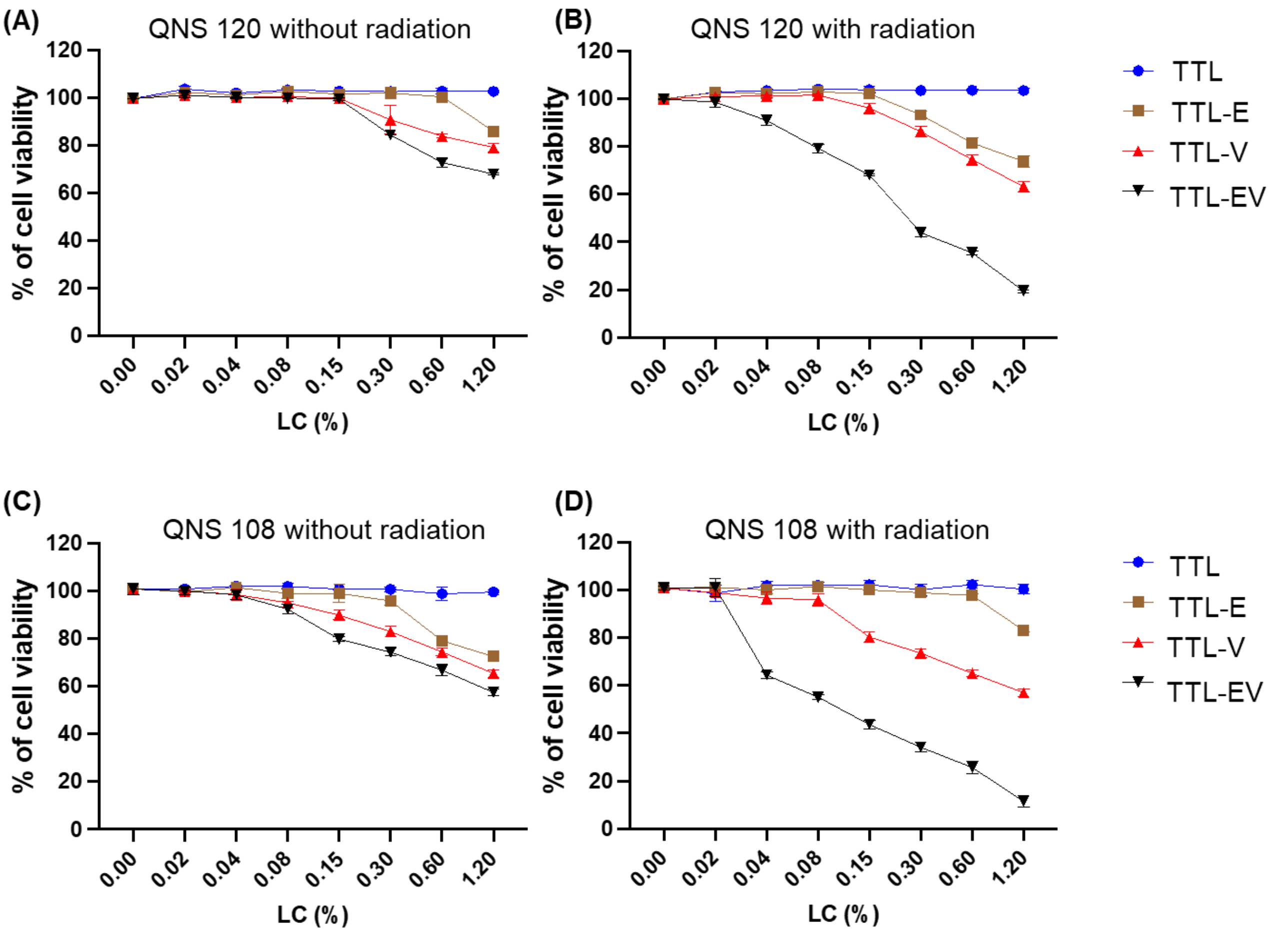

Figure S3: In vitro cytotoxicity of everolimus (E) and vinorelbine(V) loaded liposomal formulations with the combinations of both the drugs along with 2Gy of radiations in the IDH wildtype QNS120 and mutant QNS108. Then, cell viability was determined with an MTS assay. Dual drug-loaded liposomes along with the Radiation treatment showed a higher reduction in cell viability compared to dual drug-loaded liposomes in all cell lines. LC% means Liposomal concentration. 1.2% of liposomal concentration means 5 μM of everolimus and 3 μM of vinorelbine. Each data point represents the quadruplet results obtained from a single experiment. The dashed line represents the IC50 values

Table S3. IC50 concentration of the E and EV with and without radiation

Formulation	GBM 120		GBM 108	
	Without Radiation (μM)	With Radiation (μM)	Without Radiation (μM)	With Radiation (μM)
TTL-E	>5	>5	>5	>5
TTL-V	>3	>3	>3	>3
TTL-VL	>5 (E) >3 (V)	0.4±0.025 (E) 0.24±0.050 (V)	>5 (E) >3 (V)	0.25±0.08 (E) 0.15±0.09 (V)

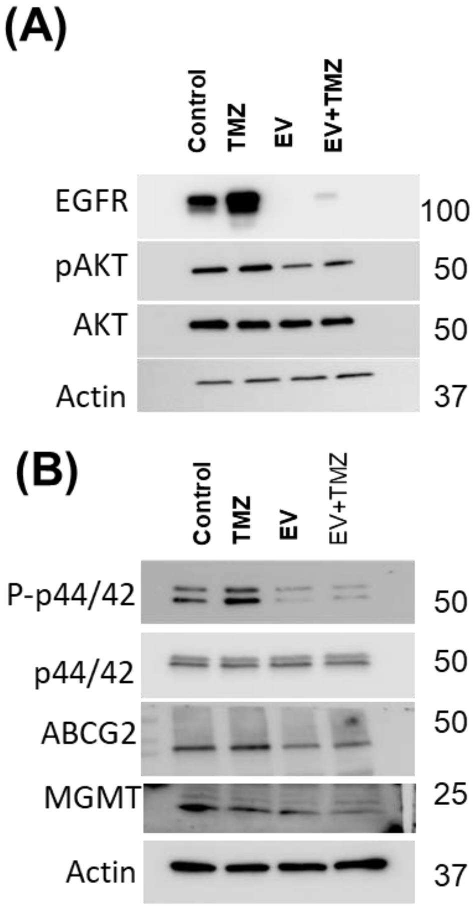

Figure S4. Western blot shows protein expression of proteins related to tumorigenesis and proliferation

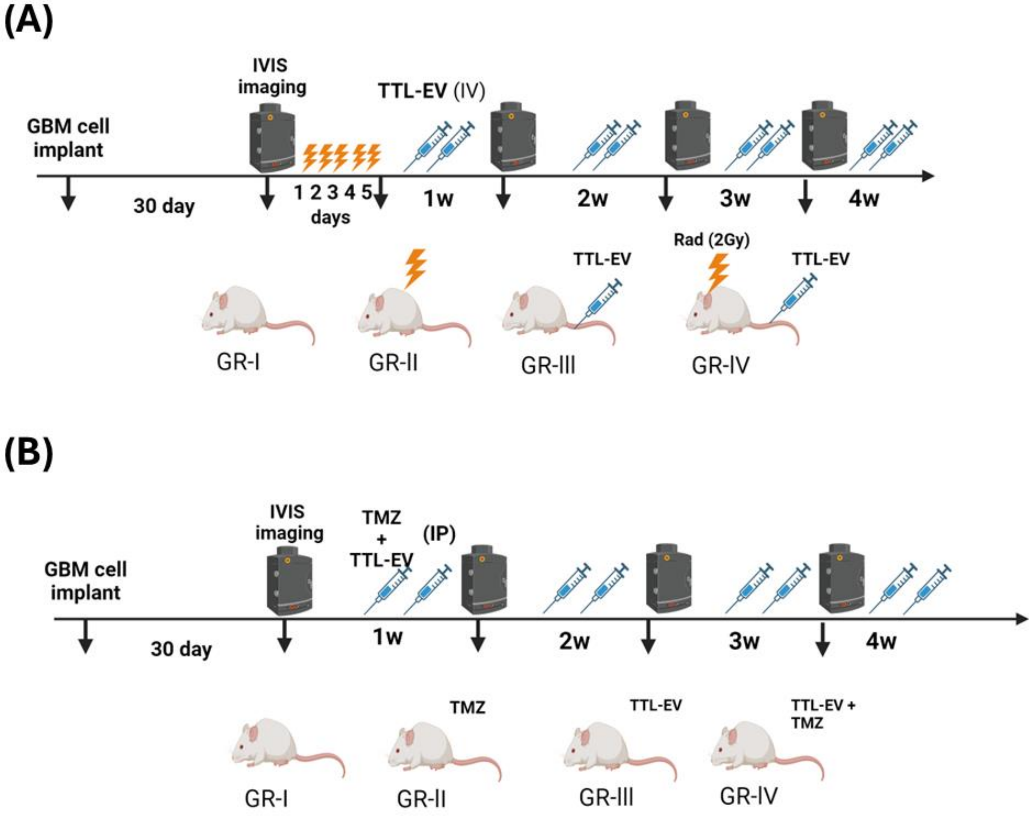

Figure S5. Schematics of the treatment: (A) TTL plus Radiation. (B) TTL-EV plus TMZ. The mice were randomized into four treatment groups. Then the mice were treated with 3.3 Gy/min radiation for five days followed by TTL-EV (equivalent doses of 2mg/Kg Everolimus, 0.95 mg/Kg Vinorelbine) 2/week for 3 weeks.

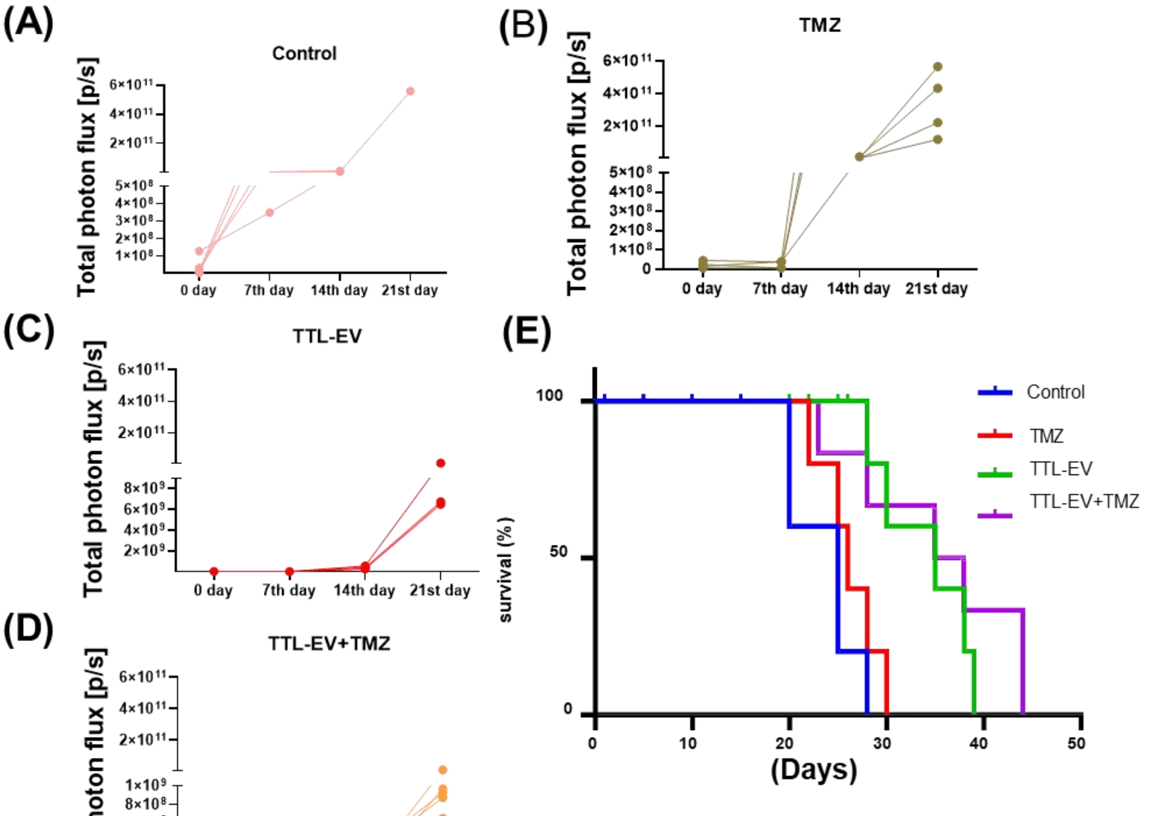

Control Vs TL-EV p<0.0039

Control Vs TL-EV +TMZ p<0.0018

(F)

Treatment groups	Median Survival (Days)
Control	23
TMZ	27
TTL-EV	39
TTL-EV+TMZ	41

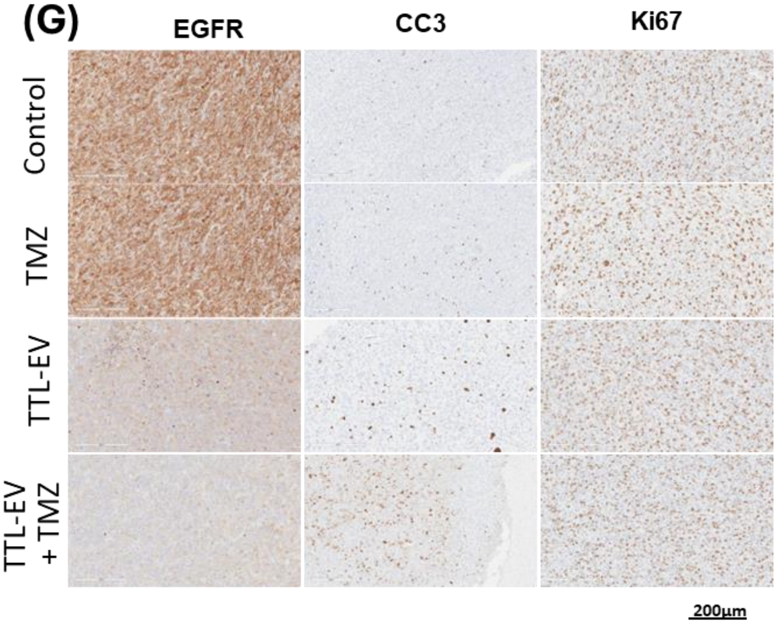

Figure S6: In vivo survival study of everolimus and vinorelbine loaded targeted liposomes with TMZ in an orthotopic glioblastoma mice tumor model. After 4 weeks of cell implantation, mice were imaged by using IVIS and randomized into four groups (n=5 in each group). Then, mice were treated with indicated groups 2/week for 3 weeks. After the end of the treatment, mice were observed, and IACUC endpoints were noted for survival analysis. **(A-D)** Tumor volume analysis across the groups. **(E)** Kaplan Meier survival plot showing median survival. **(F)** Histological analysis of mouse brain section. DAB staining for cleaved Caspase3 and Ki67. Figure represents median survival study graph developed using GraphPad software. Dose used in the present study are everolimus 1 mg/kg, vinorelbine (0.475 mg/ kg and TMZ (50 mg/Kg).

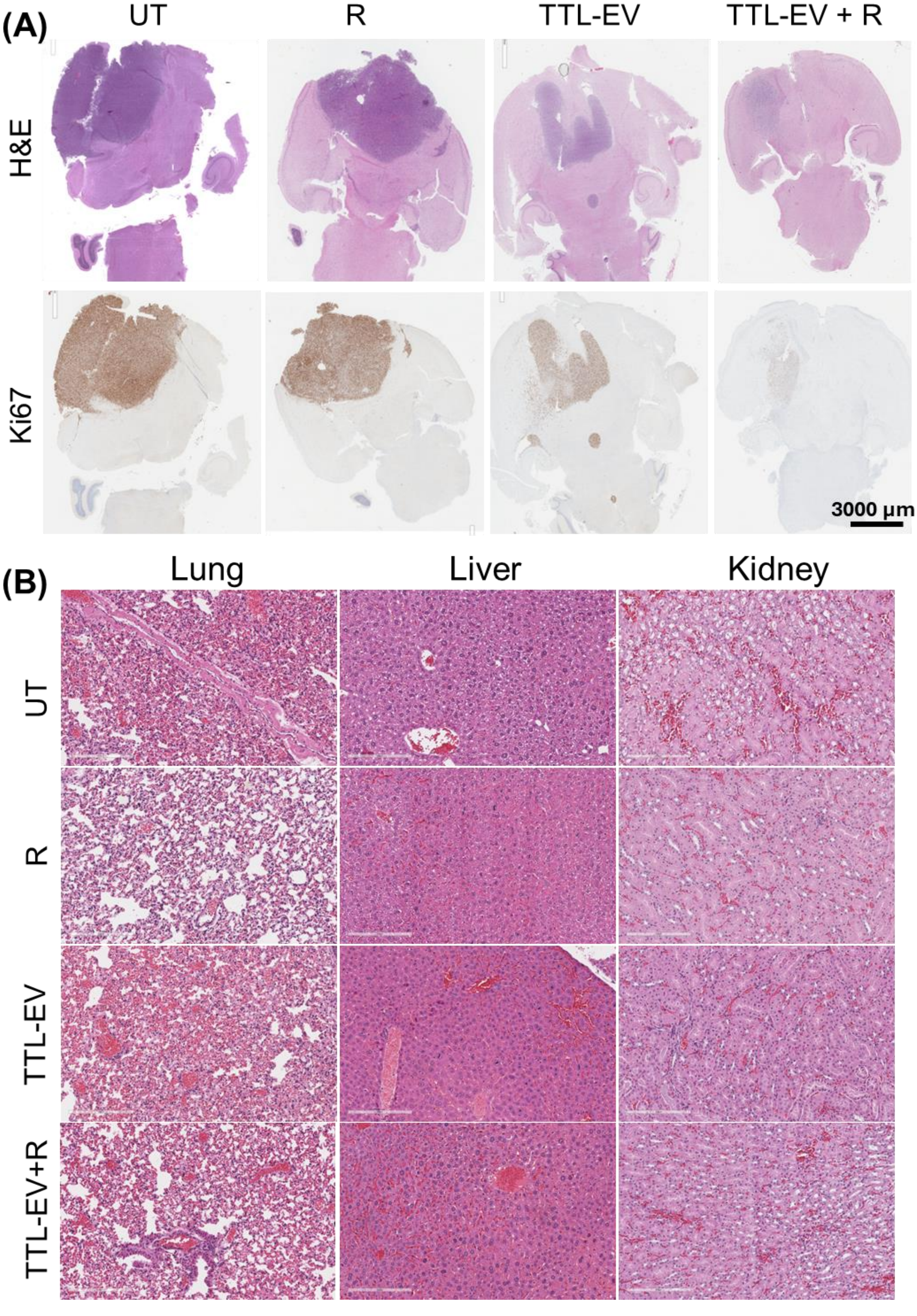
(A)
UT
R
TTL-EV
TTL-EV + R
H&E
Ki67
3000 µm
(B)
Lung
Liver
Kidney
UT
R
TTL-EV
TTL-EV+R

Figure S7. Histological Analysis of Mouse Brain and Organs.(A) Representative whole-brain sections from mice stained with hematoxylin and eosin (H&E) and Ki67 to assess tissue morphology and cell proliferation**. (B)** Representative images of the lungs, liver, and kidneys from mice in each study group: untreated (UT), radiation-treated (R), TTL-EV, and TTL-EV combined with radiation (TTL-EV + R).

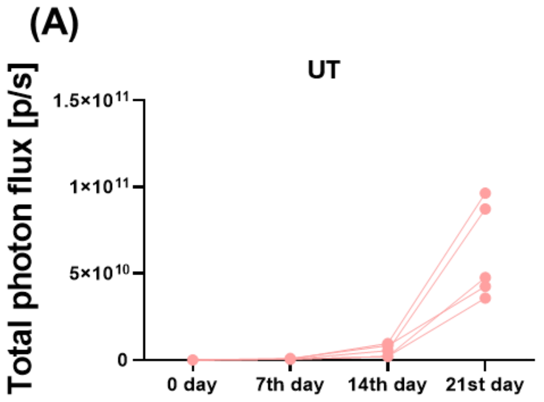

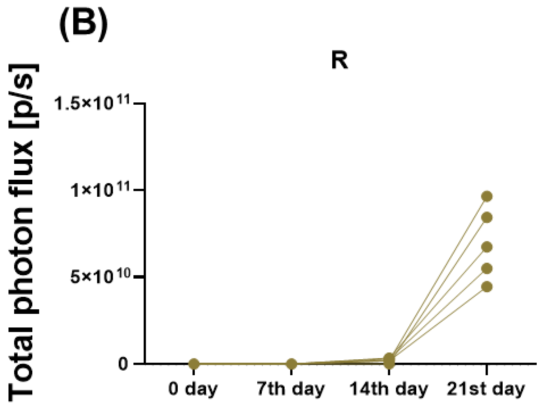

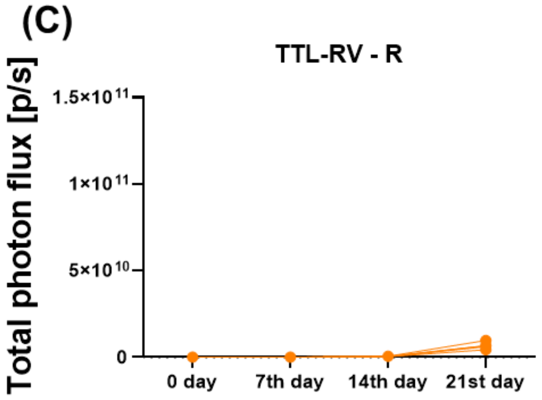

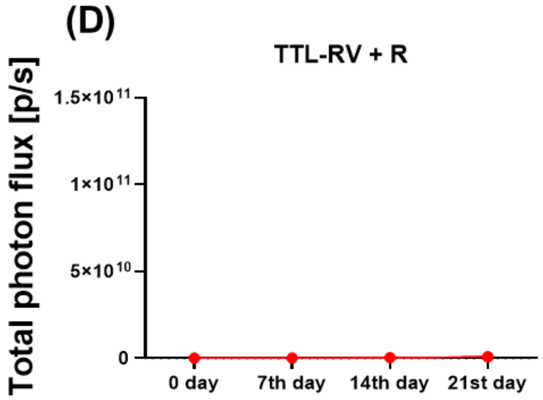

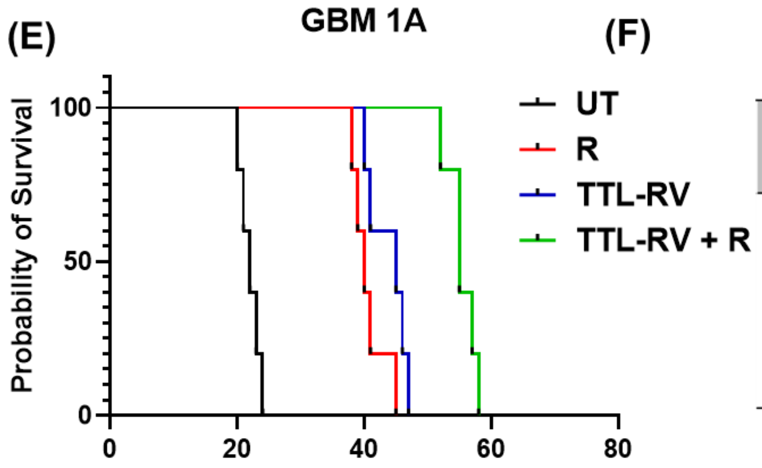

(F)

Treatment Groups	Median Survival
UT	22
R	40
TTL-RV	45
TTL-RV+R	55

UT vs R: **
UT vs TTL-RV, **
R vs TTL-RV +R, **
UT vs TTL-RV+ R**

Figure S8 : In vivo survival study of TTL_RV liposomes in combination with Radiation in an orthotopic Glioblastoma. **(A - D)** Luciferase quantification of TTL-RV, and both TTL-RV and radiation in an orthotopic GBM mice tumor model. After four weeks of cell implantation, mice were imaged using IVIS and randomized into four groups (n=5) mice per group were analyzed.. Then, mice were treated with radiation for five days, followed by TTL-RV (2mg/Kg Rapamycin, 0.95 mg/Kg Vinorelbine) 2x/week for three weeks. **(E)** In vivo survival study of rapamycin and vinorelbine-loaded liposomes (TTL-RV) and both TTL-RV and radiation in an orthotopic Glioblastoma (GBM) tumor model. **,$p<0.01$.

Table S4. Summary of RNA Sequencing Analysis

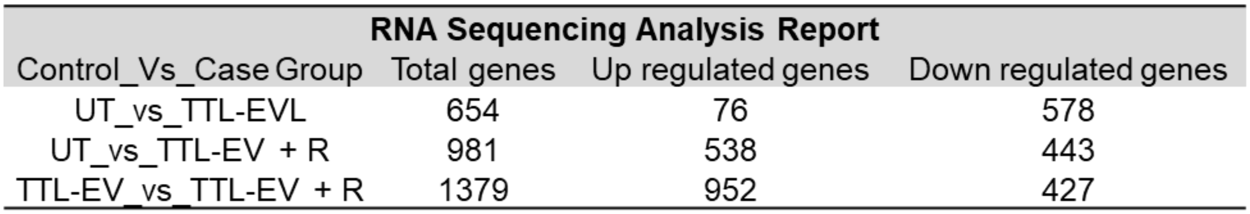

RNA Sequencing Analysis Report			
Control_Vs_Case Group	Total genes	Up regulated genes	Down regulated genes
UT_vs_TTL-EVL	654	76	578
UT_vs_TTL-EV + R	981	538	443
TTL-EV_vs_TTL-EV + R	1379	952	427

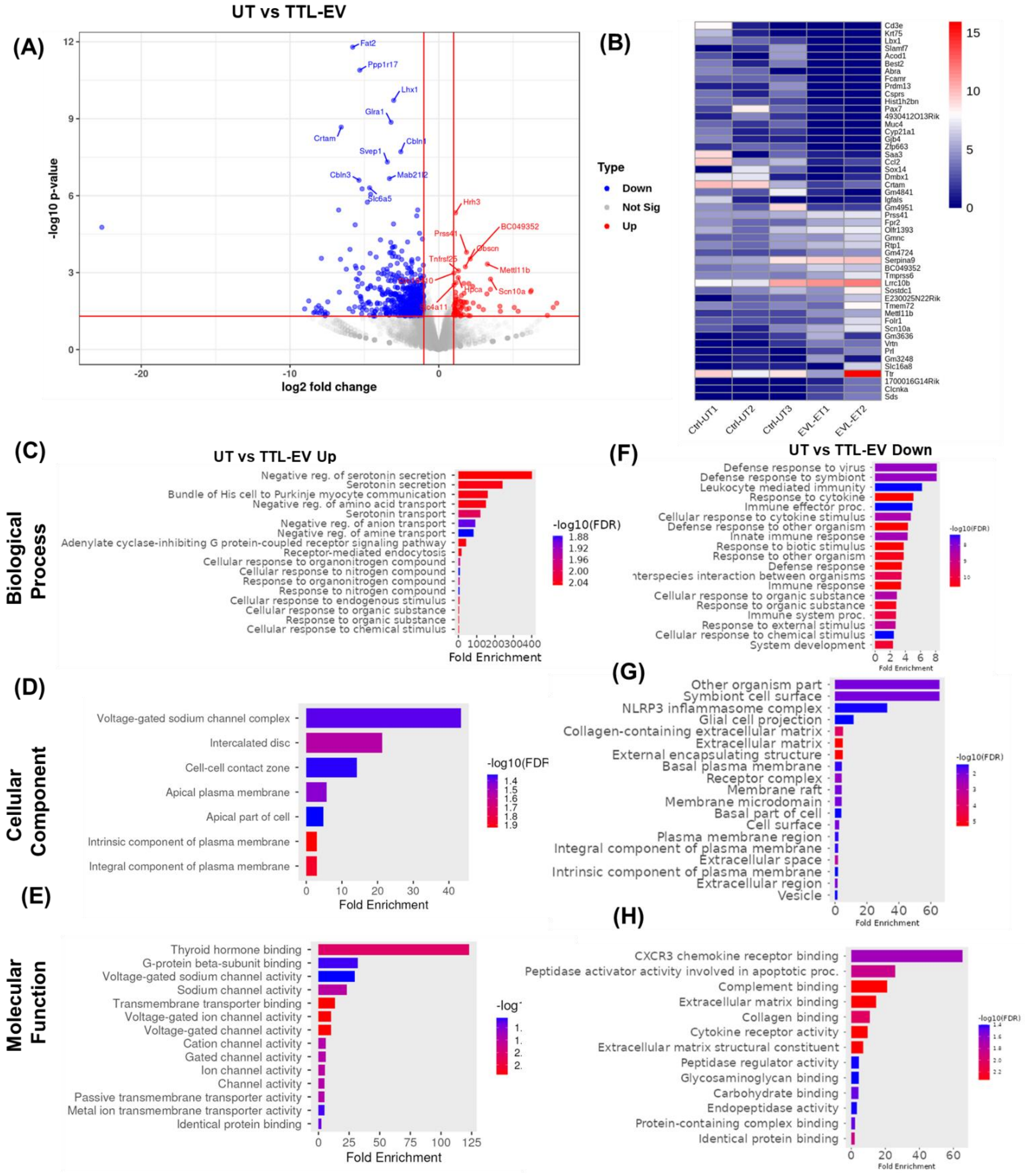

Figure S9: Transcriptome analysis in TTL-EV: (A). Volcano plot showing differentially expressed genes. **(B).** Heat map showing differentially expressed genes. **(C-E)** Gene

Ontology enrichment analysis showing: Bar plots showing the top 10 enriched ontology terms (biological processes, molecular functions, and cellular components) associated with significantly upregulated genes for the experimental conditions being compared between UT and TTL-EV, and Bar plots showing the top 10 enriched KEGG terms associated with significantly downregulated genes for the experimental conditions being compared **(F-H).**

(A)

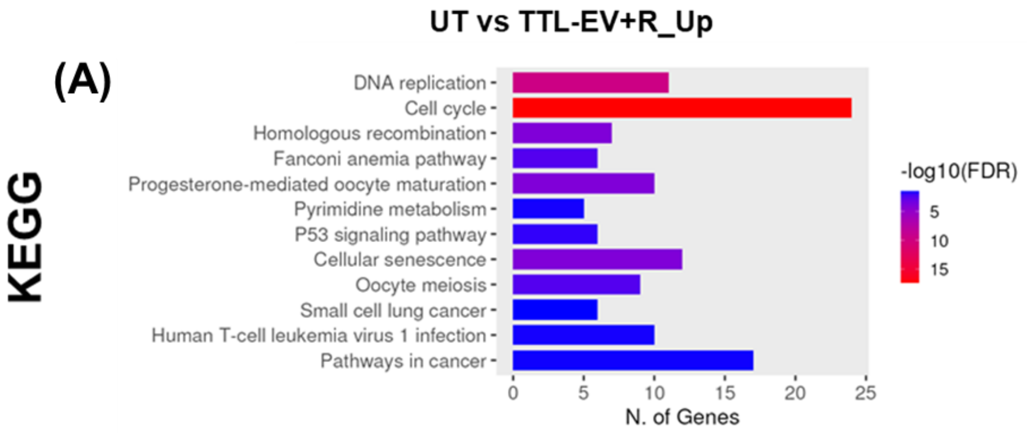
UT vs TTL-EV+R_Up
KEGG
DNA replication
Cell cycle
Homologous recombination
Fanconi anemia pathway
Progesterone-mediated oocyte maturation
Pyrimidine metabolism
P53 signaling pathway
Cellular senescence
Oocyte meiosis
Small cell lung cancer
Human T-cell leukemia virus 1 infection
Pathways in cancer
0
5
10
15
20
25
N. of Genes
-log10(FDR)
5
10
15

(C)

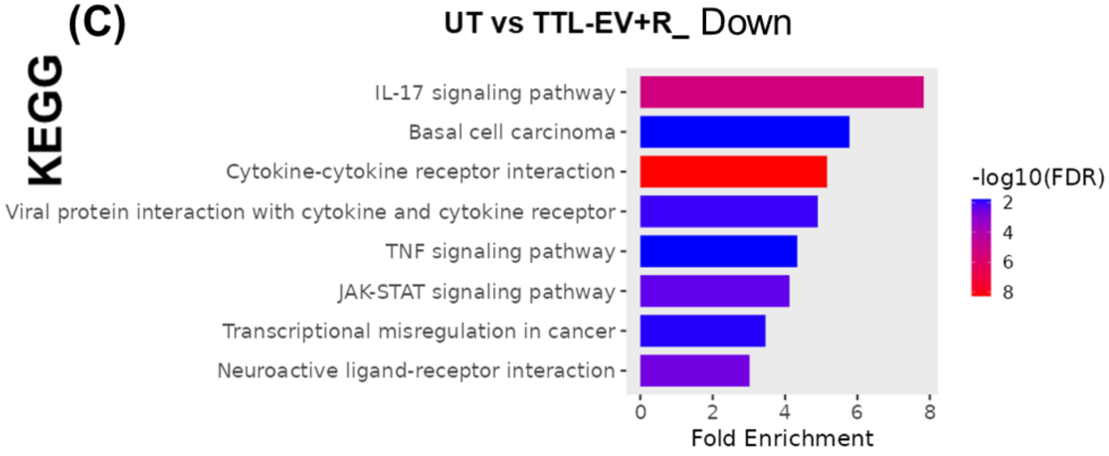
UT vs TTL-EV+R_ Down
KEGG
IL-17 signaling pathway
Basal cell carcinoma
Cytokine-cytokine receptor interaction
Viral protein interaction with cytokine and cytokine receptor
TNF signaling pathway
JAK-STAT signaling pathway
Transcriptional misregulation in cancer
Neuroactive ligand-receptor interaction
0
2
4
6
8
Fold Enrichment
-log10(FDR)
2
4
6
8

(D)

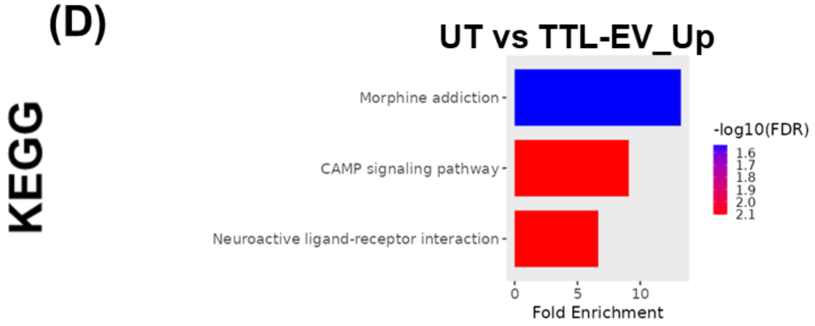
UT vs TTL-EV_Up
KEGG
Morphine addiction
CAMP signaling pathway
Neuroactive ligand-receptor interaction
0
5
10
Fold Enrichment
-log10(FDR)
1.6
1.7
1.8
1.9
2.0
2.1

(E)

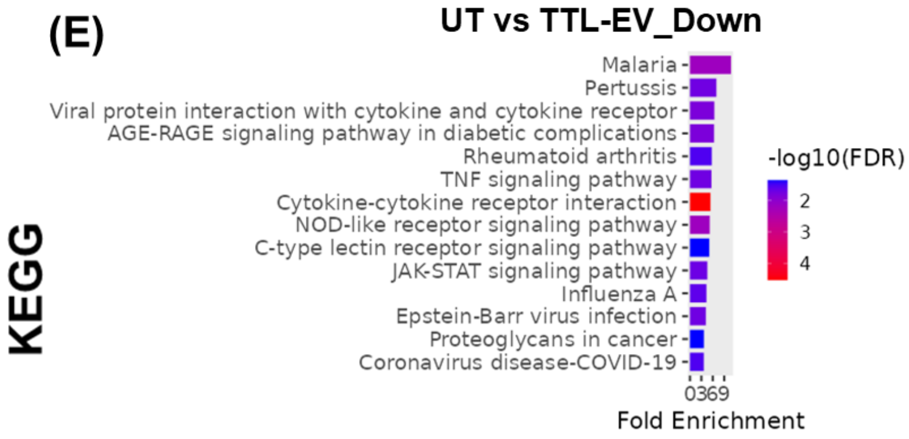
UT vs TTL-EV_Down
KEGG
Malaria
Pertussis
Viral protein interaction with cytokine and cytokine receptor
AGE-RAGE signaling pathway in diabetic complications
Rheumatoid arthritis
TNF signaling pathway
Cytokine-cytokine receptor interaction
NOD-like receptor signaling pathway
C-type lectin receptor signaling pathway
JAK-STAT signaling pathway
Influenza A
Epstein-Barr virus infection
Proteoglycans in cancer
Coronavirus disease-COVID-19
0369
Fold Enrichment
-log10(FDR)
2
3
4

Figure S10: KEGG-based gene set enrichment analysis: **(A-B)**. Bar plots showing the top 10 enriched KEGG terms associated with significantly differentially expressed genes in UT vs TTL-EV+R. **(C-D).** Bar plots showing the top 10 enriched KEGG terms associated with significantly differentially expressed genes in UT vs TTL-EV.

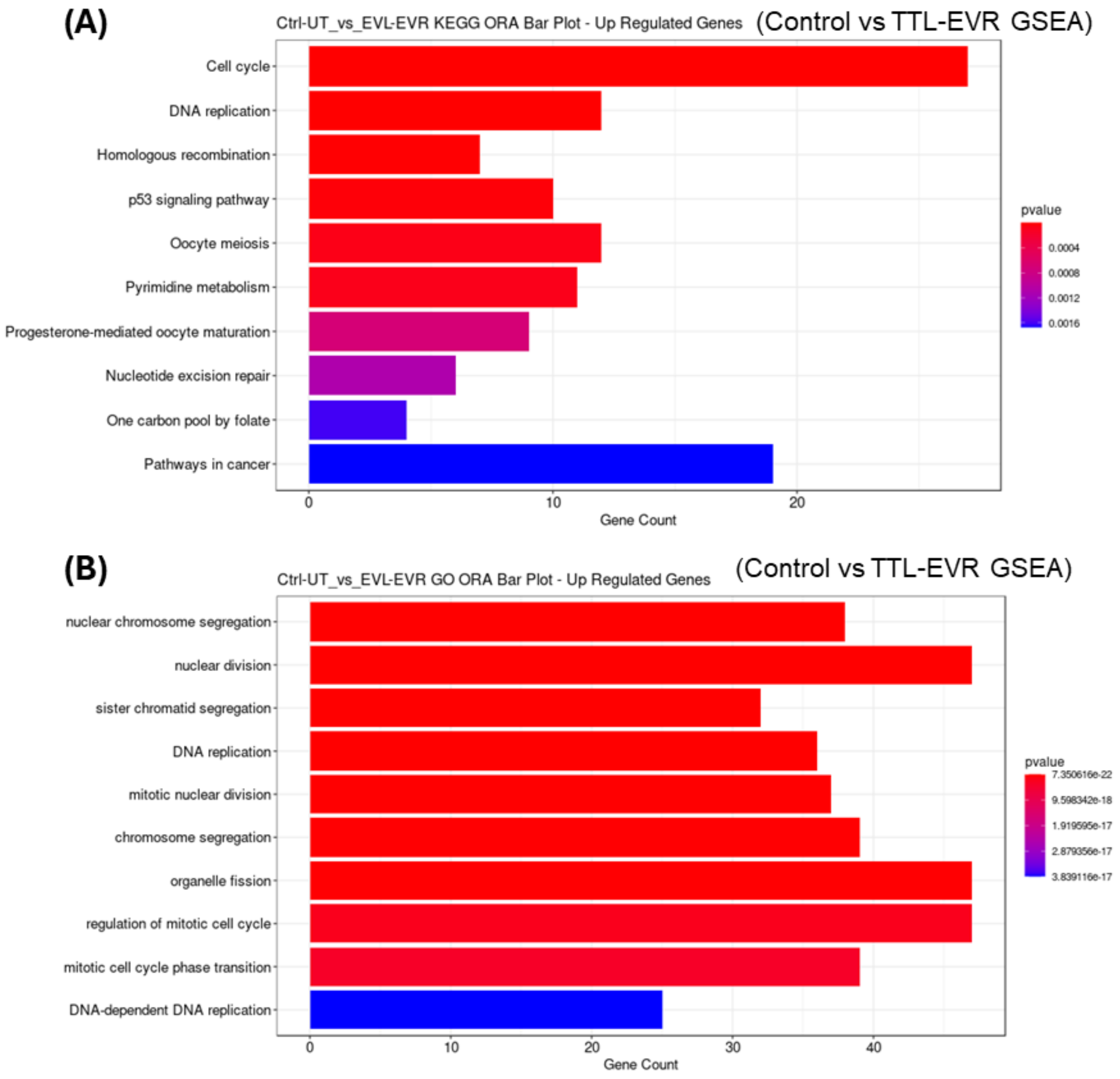

Figure S11. Bar plots showing the top 10 enriched ontology terms associated with significantly differentially expressed genes for the experimental conditions being compared. (**A**). Bar plots showing the top 10 enriched KEGG terms associated with significantly differentially expressed genes for the experimental conditions being compared. (**B**). Gene Ontology (GO) based gene set enrichment analysis: Dot plots showing the top 10 enriched GO terms associated with significantly differentially expressed genes for the experimental conditions being compared.

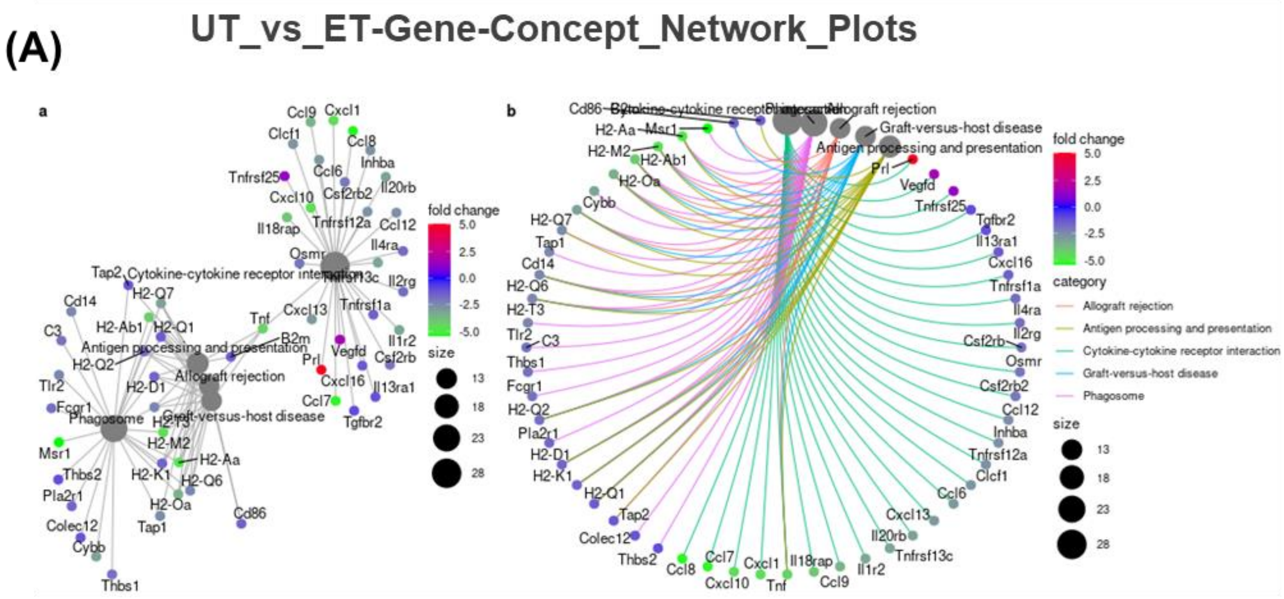

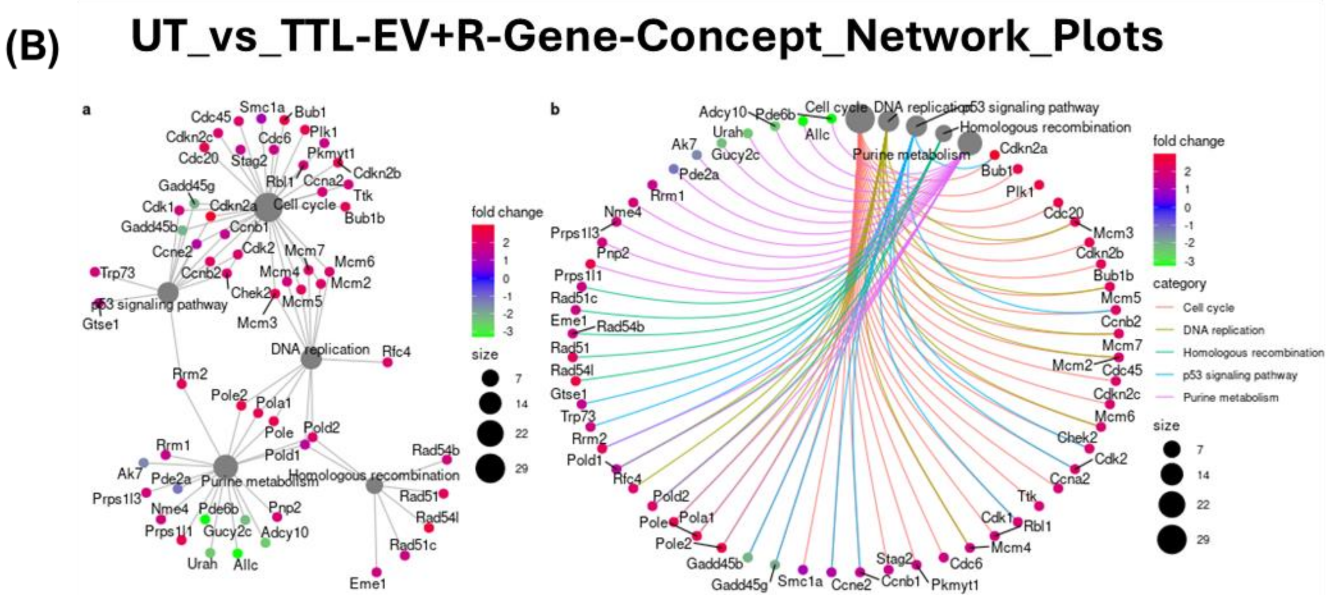

Figure S12: Gene Ontology (GO)-based overrepresentation analysis: Gene network plots depict linkages of significantly differentially expressed genes and biological GO terms. Each network plot shows the network for the top 5 GO Categories for **(A)** .UT_vs_TTL-EV-Gene-Concept_Network_Plots. **(B)** Ctrl-UT_vs_EVL-EVR-Gene-Concept_Network_Plots.

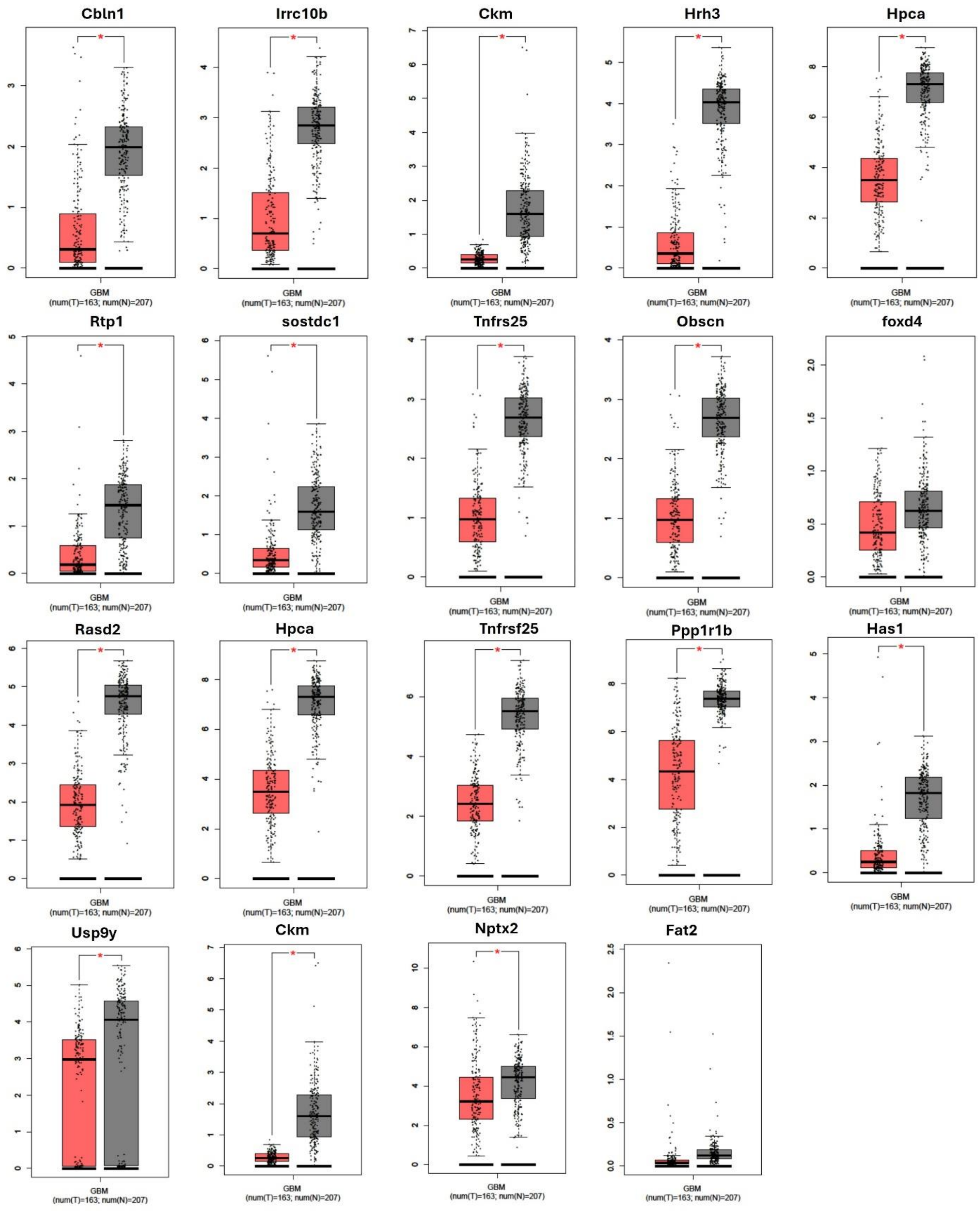
Cbln1
lrrc10b
Ckm
Hrh3
Hpca
Rtp1
sostdc1
Tnfrs25
Obscn
foxd4
Rasd2
Hpca
Tnfrsf25
Ppp1r1b
Has1
Usp9y
Ckm
Nptx2
Fat2
*
GBM
(num(T)=163; num(N)=207)

Figure S13. Evaluation of the expression of downregulated genes using GEPIA. Boxplots for the expression of the selected genes, comparing tumor and matched normal tissues in TCGA and GTEx. Y axis represents log2(TPM+1) for gene expression. The grey bar indicates the non-GBM tissues, and the red bar shows the GBM tissues. The figure were derived from GEPIA. TPM: Transcripts per million. $^*p<0.05$.Samples analyzed = 163 for Tumors (T), and 207 for Normal (N).

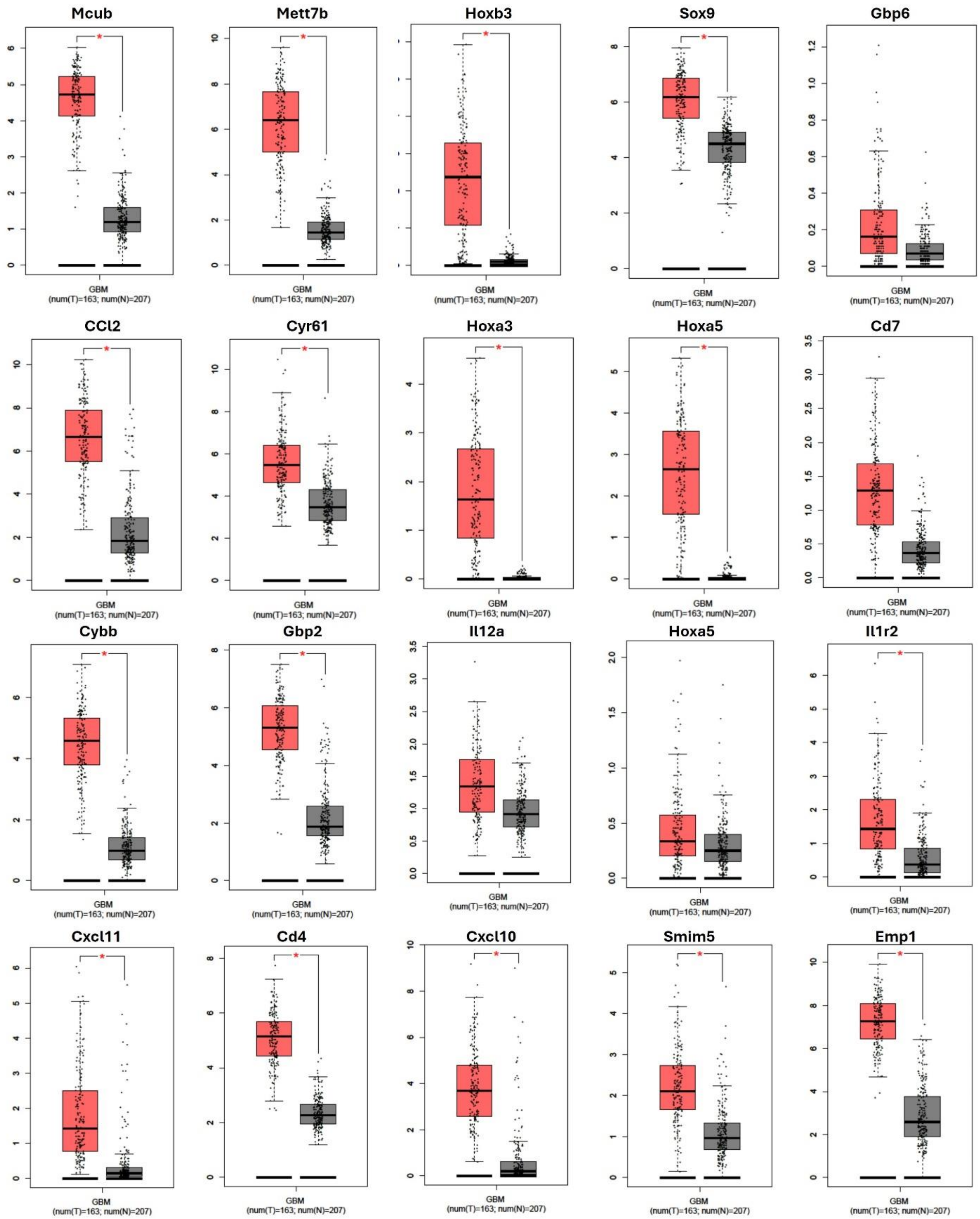
Mcub
Mett7b
Hoxb3
Sox9
Gbp6
CCl2
Cyr61
Hoxa3
Hoxa5
Cd7
Cybb
Gbp2
Il12a
Hoxa5
Il1r2
Cxcl11
Cd4
Cxcl10
Smim5
Emp1
*
GBM
(num(T)=163; num(N)=207)

Figure S14. Evaluation of the expression of the Up-regulated genes using GEPIA. Boxplots for the expression of the selected genes, comparing tumor and matched normal tissues in TCGA and GTEx. Y axis represents log2(TPM+1) for gene expression. The grey bar indicates the non-GBM tissues, and the red bar shows the GBM tissues. The figure were derived from GEPIA. TPM: Transcripts per million. $^*p<0.05$.Samples analyzed = 163 for Tumors (T), and 207 for Normal (N).

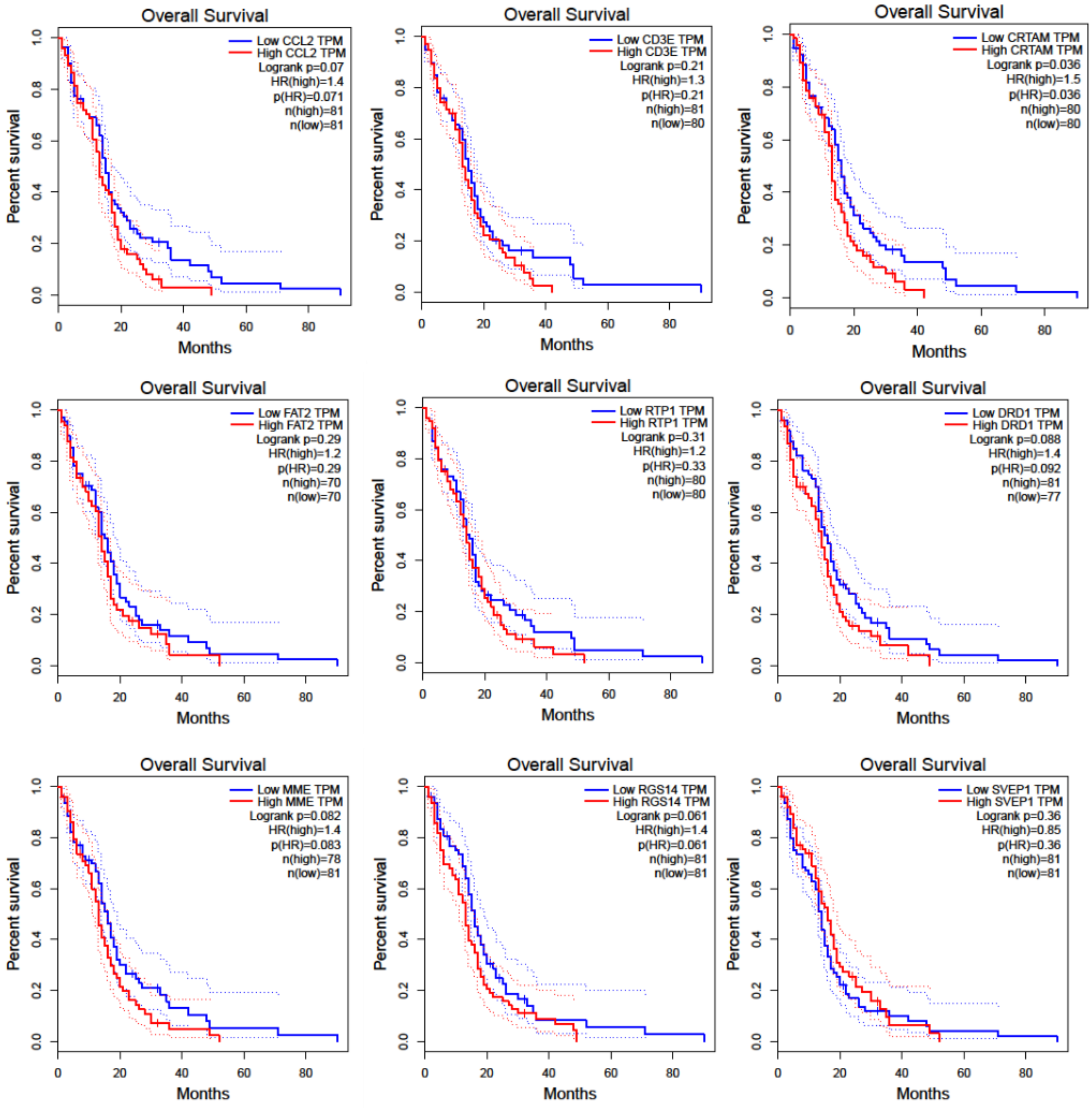

Figure S15. Kaplan-Meier analysis of the downregulated genes in the GBM mice treated TTL-EV using TCGA and GTEx dataset in GEPIA.

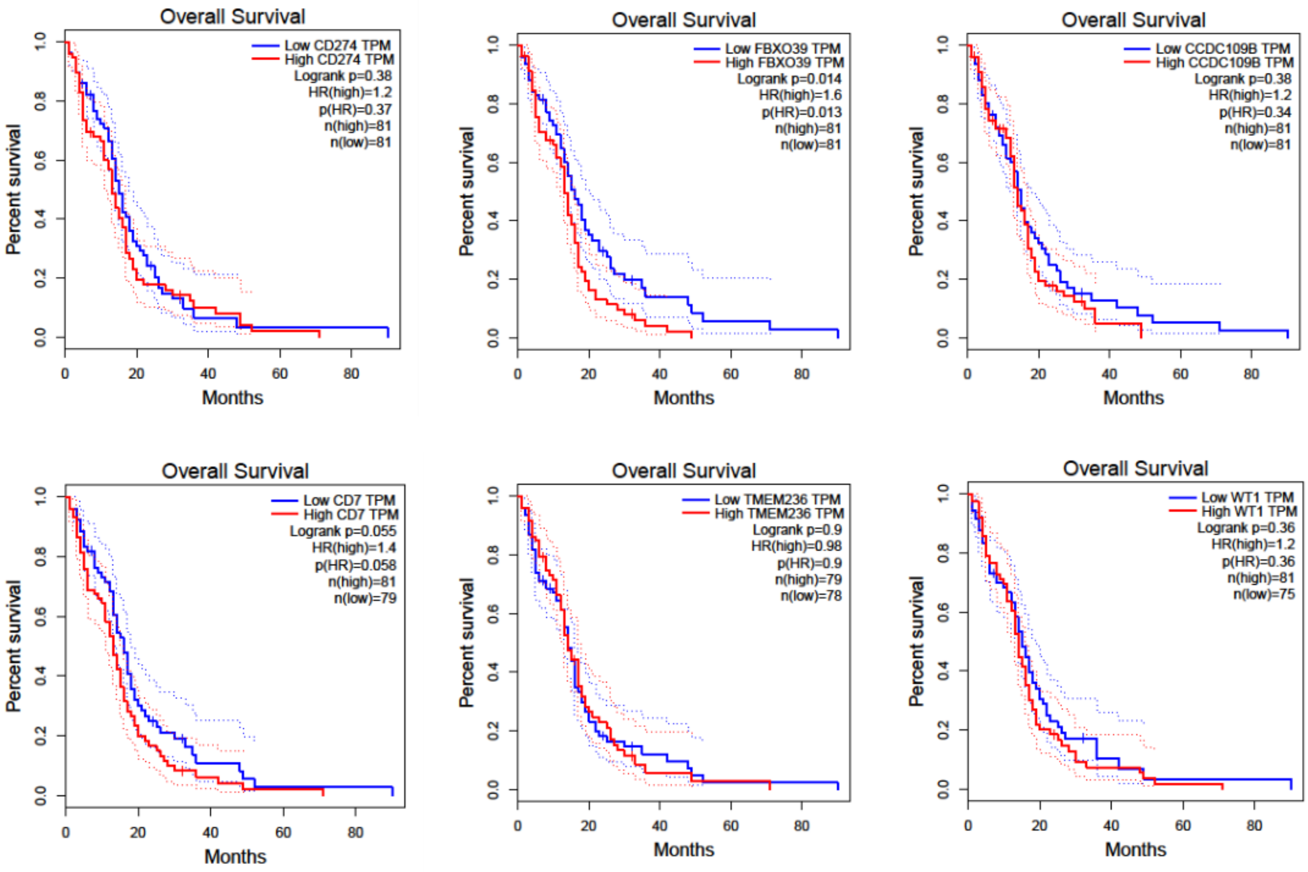

Figure S16. Kaplan-Meier analysis of the downregulated genes in the GBM mice treated TTL-EV plus EVR using TCGA and GTEx dataset in GEPIA.

Table S5: Primer List

CD3e	Forward	CTCCCCACTTCACGGAGATG
CD3e	Reverse	CCAGTTTGCCCTTAACAGTCTTG
ccl2	Forward	TTCTTCGATTTGGGTCTCCTTG
ccl2	Reverse	GTGCAGCTCTTGTCGGTGAA
ccl7	Forward	GCTGCTTTCAGCATCCAAGTG
ccl7	Reverse	CCAGGGACACCGACTACTG
cxcl10	Forward	CCAAGTGCTGCCGTCATTTTC
cxcl10	Reverse	GGCTCGCAGGGATGATTTCAA
sox14	Forward	GAAGGAGCACCCTGACTACAA
Sox14	Reverse	GGATGGCACTGGAACTAAATTGC
PDL-1	Forward	aaatggaacctggcgaaag
PDL-1	Reverse	gatgagcccctcaggcattt
Fosl1	Forward	ATGTACCGAGACTACGGGGAA
Fosl1	Reverse	CTGCTGCTGTCGATGCTTG
Msr1	Forward	TGGAGGAGAGAATCGAAAGCA
Msr1	Reverse	CTGGACTGACGAAATCAAGGAA
Pax7	Forward	TGGGGTCTTCATCAACGGTC
Pax7	Reverse	ATCGGCACAGAATCTTGGAGA
GDF3	Forward	CCGAGTTTCAAGACTCTGACC
GDF4	Reverse	CGAGCCCGGATGATTTTCCTT
Foxd4	Forward	GAGAGCCATAAGTGCCTGGAG
Foxd5	Reverse	GGAGGAGTTACTCAGATCGCC
Hoxb13	Forward	CAACGCTGATGCCAACTGTC
Hoxb14	Reverse	AGTAGCCATAAGGCACAGGAG
Cxcl17	Forward	AGGTGGCTCTTGGAAGGTG
Cxcl17	Reverse	GGTGACATCGTTTGAGAAATTGC
crtam	Forward	CACTGCATTATCCAGCACGAG
crtam	Reverse	TCAGGGGCATCTGAAGTTTCT
Hoxa9	Forward	CCCCGACTTCAGTCCTTGC
Hoxa9	Reverse	CCAGGAGCGCATATACCTGC